

## REFRIGERATION BOUND OF HEAT-PRODUCING CYLINDERS BY SUPERFLUID HELIUM

DAVID JOU <sup>a</sup>, MICHELE SCIACCA <sup>b\*</sup>, ANTONIO SELLITTO <sup>c</sup> AND LUCA GALANTUCCI <sup>d</sup>

**ABSTRACT.** In this paper we go ahead in our studies on refrigeration of nanosystems by superfluid helium, as an appealing subject for future applications to computers or astronomical precision nanodevices. We first recall the effective thermal conductivity in laminar counterflow superfluid helium through arrays of mutually parallel cylinders and we discuss the conditions for the appearance of quantum turbulence around the heat-producing cylinders. We then consider the cooling of an array of heat-producing cylindrical nanosystems by means of superfluid-helium counterflow. We discuss the upper bound on heat removal set by avoidance of quantum turbulence and avoidance of phase transition to normal He I, for arrays of cylinders placed between two infinite insulating plates and with heat flowing in the two dimensions parallel to such plates.

### 1. Introduction

One of the main applications of heat transport is for cooling heat-producing systems. Superfluid helium (He II) is one of the most efficient refrigerants because of its high thermal conductivity and its peculiarity to flow with very low viscosity and inside very narrow channels (Arp 1969; Benin and Maris 1978; Bertman and Kitchens 1968; Greywall 1981; Maris 1973; Mendelsohn 1956; Van Sciver 2012). He II is presently applied in wide channels at CERN to cool down the superconducting magnets used in particle accelerators and in narrow channels at satellites for the refrigeration of some measuring instruments, but future applications to computer nanosystems will be a further challenge. Indeed, quantum computation must be carried out at very low temperatures in order to avoid unentanglement and decoherence for as long as possible (Cirac and Zoller 1995; Di Vincenzo 2000; Suominen 2012).

In this paper we further generalize our model for refrigeration of nanosystems and of arrays of hot nano-cylinders. Jou, Galantucci, and Sciacca (2017), Saluto and Jou (2013), Saluto, Jou, and Mongiovì (2015), Sciacca and Galantucci (2016), Sciacca, Jou, and Mongiovì (2015), Sciacca *et al.* (2017), and Sciacca, Sellitto, and Jou (2014) considered heat flow in channels with different shapes of cross-section (circular and rectangular), in the presence and in the absence of quantum vortices, and for several temperatures (but below the lambda temperature for the existence of superfluidity) from a high density of heat

carriers in He II to a dilute density, where the ballistic regime becomes predominant. In all these studies we have calculated the effective thermal conductivity, in order to understand how it depends on all the parameters involved (size and shape of the channel, temperature of He II, applied heat flux, geometry of array of the transversal cylinders). One of the main results is that quantum turbulence makes the refrigerating system inefficient (Sciacca, Jou, and Mongiovì 2015), and alternative solutions are required, as for instance applying a superfluid mass flow (Jou, Galantucci, and Sciacca 2017). In particular, we obtained the maximum heat rate which may be removed from such arrays by means of the spontaneous heat counterflow. We considered that both the upper layer and lower one, as well as two lateral surfaces, were thermally insulating. Here we relax the latter assumption and allow heat flow in the two directions parallel to the upper and lower plates, and we explore in deeper detail the bounds set to avoid turbulence.

In Fig. 1, for the sake of illustration, we sketch the system we will analyze in the next sections.

The paper is organized as follows: in Section 2 we recall the mathematical model used in our papers to find the effective thermal conductivity in all the different situations considered; in Section 3 we discuss the possible appearance of quantum turbulence around the heat-producing cylinder and its effective radius; in Section 4 we apply our model and our results to find the profile of temperature of superfluid helium surrounding  $2n$  arrays of  $2m$  heat-producing cylinders; the last Section is for the conclusions.

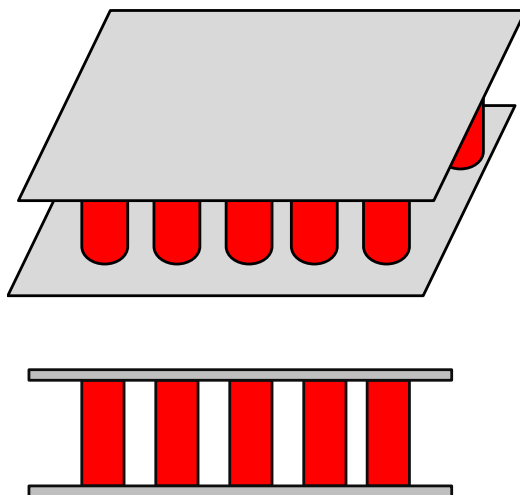


FIGURE 1. [color online] In this figure a sketch of the transversal cylinders, symmetrically distributed and surrounded by superfluid helium, is shown. The cylinders are located orthogonally to the plates and to the heat flow.

## 2. The mathematical model

The starting equations for the description of superfluid helium we are using in this paper were those obtained by means of the Extended Thermodynamics, in the one-fluid extended model, once nonlinear terms have been neglected (Jou, Lebon, and Mongiovi 2002; Jou and Mongiovi 2006; Mongiovi 1993)

$$\dot{\rho} = \rho \nabla \cdot \mathbf{v} \quad (1a)$$

$$\rho \dot{\varepsilon} = -\nabla \cdot \mathbf{q} - p \nabla \cdot \mathbf{v} + \sigma^\varepsilon \quad (1b)$$

$$\rho \dot{\mathbf{v}} = -\nabla p + \eta \nabla^2 \left( \mathbf{v} + \frac{\mathbf{q}}{ST} \right) \quad (1c)$$

$$\tau \dot{\mathbf{q}} = -\mathbf{q} - \lambda_1 \nabla T + \frac{\eta \lambda_1}{S} \nabla^2 \left( \mathbf{v} + \frac{\mathbf{q}}{ST} \right) - \tau_1 KL \mathbf{q} \quad (1d)$$

with  $\rho$  (mass density),  $\varepsilon$  (specific internal energy),  $\mathbf{v}$  (the barycentric fluid speed) and  $\mathbf{q}$  (the local heat flux) as independent variables. In the steady states, for zero net-mass flow, such equations become:

$$\nabla \cdot \mathbf{v} = 0 \quad (2a)$$

$$\nabla \cdot \mathbf{q} = \sigma^\varepsilon \quad (2b)$$

$$\nabla p - \eta \left( \nabla^2 \mathbf{v} + \frac{\nabla^2 \mathbf{q}}{ST} \right) = \mathbf{0} \quad (2c)$$

$$\lambda_1 \nabla T - \frac{\eta \lambda_1}{S} \left( \nabla^2 \mathbf{v} + \frac{\nabla^2 \mathbf{q}}{ST} \right) = -\mathbf{q} (1 + \tau_1 KL). \quad (2d)$$

In Eqs. (2)  $S$  means the entropy per unit volume,  $p$  pressure,  $T$  temperature,  $\tau_1$  the relaxation time of  $\mathbf{q}$ ,  $\sigma^\varepsilon$  the local energy supply (which in our case will be the heat dissipated by the cylinders of the array being considered), and  $\lambda_1$  and  $\eta$  can be interpreted as the thermal conductivity and the shear viscosity, respectively, when applied to a classical fluid (Mongiovi 1993). The two coefficients  $\lambda_1$  and  $\tau_1$  can be related to the second-sound speed  $w_2$  by

$w_2 = \sqrt{\frac{\lambda_1}{\tau_1 \rho C_v}}$ , being  $C_v$  the specific heat per unit mass at constant volume (Mongiovi 1993). In Eq. (2d)  $L$  is the vortex length density of quantum turbulence, for which we do not consider a dynamical equation, because we are interested only to laminar situation (i.e. in absence of quantum turbulence),  $K$  is a friction coefficient describing the resistance of the vortex tangle to the heat flow. Sciacca, Jou, and Mongiovi (2015) have considered the quantum Reynolds number

$$\text{Re}_q = \frac{(\rho/\rho_s)(q/ST)d}{\kappa} \quad (3)$$

with  $\kappa$  is the quantum of circulation (i.e.,  $\kappa = h/m_{\text{He}} \equiv 9.97 \times 10^{-8} \text{ m}^2 \text{ s}^{-1}$ , with  $h$  being the Planck's constant, and  $m_{\text{He}}$  the atomic mass of helium),  $d$  means the smallest size of the channel wherein He II flows. Quantum Reynolds number is useful to establish the thresholds for the appearance of quantum turbulence ( $\text{Re}_1$  for TI turbulence and  $\text{Re}_2$  for TII turbulence) (Jou and Sciacca 2013). When  $\text{Re}_q$  is of the order of 100 (the exact value depends on temperatures), quantum turbulence appears.

In the laminar regime Eqs. (2c) and (2d) become as in (Sciacca and Galantucci 2016; Sciacca, Jou, and Mongiovi 2015; Sciacca *et al.* 2017; Sciacca, Sellitto, and Jou 2014)

$$\nabla p = \left( \frac{\eta}{ST} \right) \nabla^2 \mathbf{q} \quad (4a)$$

$$-S\nabla T + \nabla p = \left( \frac{S}{\lambda_1} \right) \mathbf{q} \quad (4b)$$

because the contribution arising from  $\nabla^2 \mathbf{v}$  can be removed once the averaged fields are considered and the counterflow condition ( $\bar{\mathbf{v}} = 0$ ) is applied (see Sciacca, Jou, and Mongiovi 2015 for more details).

Equations (4) have been used to study heat transport in He II laminar counterflow along cylindrical tubes (Sciacca, Jou, and Mongiovi 2015; Sciacca, Sellitto, and Jou 2014) and channels with a rectangular transversal section (Sciacca and Galantucci 2016). Below, we briefly report some of the main results by Sciacca *et al.* (2017), that take into account the presence of arrays of cylinders (whose vertical axes are perpendicular to the direction of the flow) and which are mimicking in a simplified way heat-dissipating nano-chips (for instance). The heat flowing through the lattice of transversal cylinders we are considering is also sketched in Fig. 2, where  $R$  and  $2c$  stand for the radius of each cylinder and the distance between the axes of two consecutive cylinders.

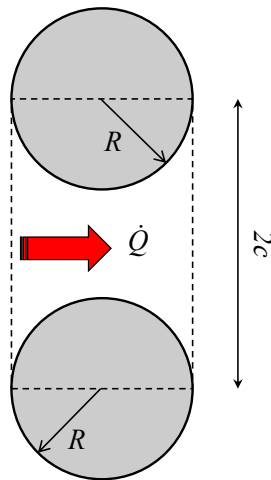


FIGURE 2. [color online] The total heat flux  $\dot{Q}$  (arrow) flowing through two consecutive cylinders in the arrays of transversal cylinders symmetrically distributed over the channel.

Let us also consider a  $2c \times 2c$  elementary cell and set  $\phi = R/c$ . The pressure drop in the direction of the applied heat flux between the two points in front and behind the cylinders

has been calculated by Sciacca *et al.* (2017) as

$$\begin{aligned} \Delta p &= p(-c) - p(c) = \\ &= \frac{3\eta\dot{Q}}{2bc^2ST} \left\{ 2(1-\phi) + \frac{\phi^2}{(1-\phi^2)^{5/2}} \left[ \frac{3\pi}{2} + \frac{(2+\phi^2)}{\phi} \sqrt{1-\phi^2} + 3 \arctan \left( \frac{\phi}{\sqrt{1-\phi^2}} \right) \right] \right\} \end{aligned} \quad (5)$$

and the corresponding  $\Delta T$  (obtained by means of  $\Delta p = S\Delta T$ ) is

$$\Delta T = \frac{3\eta\dot{Q}}{2bc^2S^2T} \left\{ 2(1-\phi) + \frac{\phi^2}{(1-\phi^2)^{5/2}} \left[ \frac{3\pi}{2} + \frac{(2+\phi^2)}{\phi} \sqrt{1-\phi^2} + 3 \arctan \left( \frac{\phi}{\sqrt{1-\phi^2}} \right) \right] \right\}. \quad (6)$$

Two main limiting situations are worth of consideration:  $1-\phi \ll 1 \Leftrightarrow \phi \rightarrow 1$  (the spacing between the cylinders is much smaller than their cross-sectional dimensions) and  $\phi \ll 1 \Leftrightarrow \phi \rightarrow 0$  (the spacing between the cylinders is much larger than their radius  $R$ ). In these cases, Eq. (6) can be further simplified in order to get the following expressions of temperature difference and of the corresponding effective thermal conductivity:

(1)  $1-\phi \ll 1 \Leftrightarrow \phi \rightarrow 1$ :

$$\Delta T = \frac{9\pi\eta\dot{Q}}{2bc^2S^2T} \left[ \frac{\phi^2}{(1-\phi^2)^{5/2}} \right] \quad (7)$$

and hence the effective thermal conductivity for He II is

$$K_{\text{eff}} = \frac{\dot{Q} l}{A \Delta T} = \frac{2c^2S^2T}{9\pi\eta(1-\phi)} \left[ \frac{\phi^2}{(1-\phi^2)^{5/2}} \right]^{-1}, \quad (8)$$

where the length  $l = 2c$  and the transversal area is  $A = 2cb(1-\phi)$ .

(2)  $\phi \ll 1 \Leftrightarrow \phi \rightarrow 0$ :

$$\Delta T = \frac{3\eta\dot{Q}}{bc^2S^2T} \quad (9)$$

and the effective thermal conductivity for He II is

$$K_{\text{eff}} = \frac{c^2S^2T}{3\eta(1-\phi)} \quad (10)$$

The local value of the heat flux may be described as  $\mathbf{q} = -K_{\text{eff}}\nabla T$ , with  $K_{\text{eff}}$  given by Eq. (8) or (10), or by the general expression obtained from (6), if the simplifications  $\phi \rightarrow 0$  or  $\phi \rightarrow 1$  do not apply. Though  $\mathbf{q} = -K_{\text{eff}}\nabla T$  has obviously the aspect of the usual Fourier law, note that it emerges from much more complicated model (1), after a cumbersome integration and average has been carried out. The fact that in the situation considered here Eq. (4) leads to an effective Fourier's law cannot be extrapolated to any situation. For instance, in the case of heat flowing radially from a single cylinder or a single sphere, the law relating  $\mathbf{q}$  to the local value of the temperature gradient may be very different from that of Fourier's law.

It would be also interesting to analyze how the effective thermal conductivity changes with other geometrical details, as for instance if instead of cylinders the dissipating devices have a square or rectangular form. This will be the aim of a forthcoming paper.

### 3. Appearance of quantum turbulence around the cylinder

In this section we are interested to investigate a possible appearance of quantum turbulence around a “hot” cylinder of radius  $R$  and height  $b$  which delivers heat to the surrounding He II. To this end, let us assume that the cylinder produces a radial heat flux  $q(r) = \frac{\dot{Q}}{2\pi r b}$  for  $r \geq R$ , with  $r$  as the distance from the axis of the cylinder. The quantum Reynolds number is a function of the heat flux according to Eq. (3), i.e.,

$$\text{Re}_q = \left( \frac{\rho}{\rho_s T S} \right) \left( \frac{\dot{Q}}{2\pi r b} \right) \left( \frac{d}{\kappa} \right) \quad (11)$$

In particular, in the present case it decreases for increasing  $r$ , for a given value of  $d$ . Here we will take  $d \approx b$  for the sake of simple estimation (as it will be commented below, in an array of cylinders, one could take  $d$  as the minimum of the cylinder length  $b$  and of their mutual separation). Because of the strong dependence of  $\text{Re}_q$  on  $r$  in the geometry considered here, quantum turbulence could appear next to the walls of the cylinder for  $\text{Re}_q(r) \geq \text{Re}_1$  for  $R \leq r \leq \bar{r}$ . The maximum  $\bar{r}$  for which  $\text{Re}_q(r) \geq \text{Re}_1$  is given by

$$r_1 = \text{Re}_1^{-1} \left( \frac{\rho}{\rho_s} \right) \left( \frac{1}{2\pi} \right) \left( \frac{\dot{Q}}{T S \kappa} \right) \quad (12)$$

whereas He II is in the laminar regime for  $r \geq r_1$ . It also could occur that the dissipated heat in the cylinder is so high that  $\text{Re}_q(r) > \text{Re}_2$ . In this case we can find two critical radii,  $r_2$  and  $r_1$ , such that He II exhibits quantum turbulence in the state TII in the region  $R \leq r \leq r_2$ , in the state TI in the region  $r_2 \leq r \leq r_1$  and laminar regime for  $r \geq r_1$ .

The gap  $\Delta T$  in the turbulent regimes is higher than that in the laminar regime because  $\Delta T = \Delta T_{\text{lam}} + \Delta T_{\text{turb}} \geq \Delta T_{\text{lam}}$ , and it is higher for higher values of the vortex line density  $L$ , and hence in the state TII than in the state TI.

In the turbulent regime ( $R \leq r \leq r_1$ ) the temperature gap  $\Delta T$  is so high because part of the energy is supplied to the quantum vortex tangle to keep it on. In the laminar regime, instead, all the heat goes away from the cylinder without any dissipation against the quantum vortices. Because the vortex tangle acts as a resistance where energy is dissipated, the turbulent region can be imagined as part of a wider cylinder with an effective radius given by  $r_{\text{eff}} \sim r_1$ . Indeed, considering that part of the energy is locked in the vortex tangle the effective “hot” cylinder is not the one of radius  $R$ , but that of radius  $r_{\text{eff}}$ , which include the cylinder and the turbulent region of He II around it. In this case the radius of the cylinder would become

$$r_{\text{eff}} \equiv \text{Re}_1^{-1} \left( \frac{\rho}{\rho_s} \right) \left( \frac{1}{2\pi} \right) \left( \frac{\dot{Q}}{T S \kappa} \right) \quad (13)$$

in such a way that the new Reynolds number would be smaller than the critical value  $\text{Re}_1$ . A higher radius of the cylinder would mean a higher  $\phi$  in the expression of the effective thermal conductivity, as well as a smaller spacing between the cylinders  $2c(1 - \phi)$ . From Eqs. (8) and (10) we note that the effective thermal conductivity in the presence of quantum turbulence around the cylinders  $K_{\text{eff}}^t$  would be smaller for  $r_{\text{eff}} > R$ , namely

$$K_{\text{eff}}^t < K_{\text{eff}}$$

In the previous section we have applied our mathematical model to calculate the effective thermal conductivity through the gap between two cylinders with radius  $R$ ,  $2(c - R)$  spacing, and height  $b$ . Then we have distinguished two main situations: large spacing in Eq. (10) and narrow spacing in Eq. (8) between cylinders, as also studied by Sciacca *et al.* (2017). There, indeed, some arrays of heat-producing cylinders were symmetrically distributed in a rectangular channel with the axis orthogonal to the mean flow and to the plates of the channel.

Saluto, Jou, and Mongiovi (2014) and Sciacca *et al.* (2017) considered heat-producing cylinders. One of the main drawbacks which may arise in the refrigeration is the appearance of quantum turbulence around the cylinder. Indeed, if the heat produced by the cylinder is  $\dot{Q}$  then the radial heat flux is  $q(r) = \frac{\dot{Q}}{2\pi r b}$  for  $r \geq R$ , with  $r$  as the distance from the axis of the cylinder. If  $\dot{Q}$  is high enough then quantum turbulence may appear around the “hot” cylinder.

More in details, let  $\text{Re}_1$  be the critical Reynolds number for the appearance of TI turbulence (mild turbulence in He II) then the condition for having quantized vortices around the cylinder up to  $r'$  is that

$$\text{Re}_q = \frac{\rho}{\rho_s} \frac{(q(r')/ST)d}{\kappa} > \text{Re}_1 \quad (14)$$

with  $q(r') = \frac{\dot{Q}}{2\pi r' b}$ . From (14) we can state that He II around the cylinder is free-vortex if  $r' = R$ .

We can also estimate the thickness,  $r_{\text{eff}} - R$ , of the layer of quantum turbulence around the cylinder for a given heat-produced  $\dot{Q}$ , namely

$$r_{\text{eff}} - R \equiv \text{Re}_1^{-1} \left( \frac{\rho}{\rho_s} \right) \left( \frac{1}{2\pi} \right) \left( \frac{\dot{Q}}{TS\kappa} \right) - R, \quad (15)$$

and the laminar case is expected for  $r_{\text{eff}} - R = 0$ .

If the produced  $\dot{Q}$  is not low enough then some alternative strategies have to be considered for cooling the system. One of them is surely the application of an external mass flow for removing heat as well as quantized vortices from the surface of the cylinders.

In any strategy that may be implemented, we have to consider that our cylinders will have an effective radius  $r_{\text{eff}}$  higher than  $R$  because quantum turbulence keeps heat as it were part of the cylinder. Thus, the radius to be considered in the Eqs. (8) or (10) is  $r_{\text{eff}}$ , and not the actual radius  $R$ . It means that in the case of high enough  $\dot{Q}$  produced by cylinders with small radius  $R$ , the effective radius  $r_{\text{eff}}$  would be high enough that  $K_{\text{eff}}$  becomes Eq. (8), namely, the effective thermal conductivity for small spacing between the cylinders.

Instead, if  $\dot{Q}$  is so high to produce quantum turbulence around the cylinders in the case 1, (namely  $1 - \phi \ll 1 \Leftrightarrow \phi \rightarrow 1$ ) then the effective radius of the cylinders is further reduced inhibiting much more the efficiency of the refrigerating system, as commented by Sciacca *et al.* (2017). One could wonder what is the maximum value of  $\dot{Q}$ , produced by each cylinder, to make He II completely turbulent? The answer to this question is simple because it occurs when  $r_{\text{eff}} = c$ , namely when the sum of the effective radius of two consecutive cylinders is exactly the distance between their axis and hence the spacing between the

cylinders is null. More explicitly, from Eq. (15) it follows

$$\dot{Q}_{\max} = 2c\text{Re}_1TS\kappa\frac{2\pi\rho_s}{\rho} \quad (16)$$

which is the condition that  $r_{\text{eff}} = c$ . Note that this value for  $\dot{Q}_{\max}$  refers to the heat dissipated by a single cylinder. In the next section we will also derive the total  $\dot{Q}_{\max}$  that may be removed from the system. It would be of interest to apply these results to a quantum computer with  $n \times n$  qubits, each of them consisting for instance of a magnetic ion.

In the above estimations we have always assumed that the heat-produced  $\dot{Q}$  is such that the temperature is smaller than the lambda temperature in order to avoid that He II becomes He I, as stated by Mongiovì and Saluto (2014).

#### 4. Application to refrigeration of arrays of heat-producing cylindrical nanosystems

In this section we apply the above results to the refrigeration of arrays of heat-producing cylinders, each of them assumed to dissipate an energy  $\dot{Q}_{ij}$  (with the subscripts  $i$  and  $j$  indicating the column and the row where the cylinder is found) per unit time as the consequence of its internal functioning. Now we want evaluate the profile of the temperature inside the lattice of cylinders. In order to keep the system efficient, the total power  $\dot{Q}_{\text{tot}} = \sum_{i,j} \dot{Q}_{ij}$  produced by all the cylinders must be removed.

Following the same procedure used by Sciacca *et al.* (2017), we consider  $2n$  columns of  $2m$  cylinders symmetrically arranged (see Fig. 3 for a qualitative sketch of the geometry). For the sake of illustration let us assume that the origin of the reference frame is in the middle of the columns and of the rows, with the subindices  $i$  and  $j$  denoting the position (i.e., the row and the column) of the cylinder in the array in such a way that  $j = -n \dots, -1, 1, \dots, n$  and  $i = -m \dots, -1, 1, \dots, m$ . Furthermore, we assume that each cylinder delivers the same amount of heat per unit time, i.e.,  $\dot{Q}_{ij} = \dot{Q}$ .

Now, we evaluate the temperature gap  $\Delta T_{j,j+1}^i$  through the cylinders located at  $(i, j)$  and  $(i, j+1)$ :

$$\begin{aligned} \Delta T_{j,j+1}^i &= (T_i^s - T_i^c) + (T_i^c - T_{i-1}^s) = T_i^s - T_{i-1}^s = \\ &= \sum_{k=i+1}^n K_{\text{eff}}^{-1} \left( \frac{\dot{Q}_k}{2} \right) - \sum_{k=-n}^{i-1} K_{\text{eff}}^{-1} \left( \frac{\dot{Q}_k}{2} \right) = - \left( i - \frac{1}{2} \right) K_{\text{eff}}^{-1} \dot{Q}' \end{aligned} \quad (17)$$

where  $\dot{Q}' = \dot{Q}/4$  because we assume that heat produced by the cylinders is radiated isotropically.

In analogous way, the temperature gap  $\Delta T_{i,i+1}^j$  through the cylinders located at  $(i, j)$  and  $(i+1, j)$  is:

$$\begin{aligned} \Delta T_{i,i+1}^j &= (T_j^s - T_j^c) + (T_j^c - T_{j-1}^s) = T_j^s - T_{j-1}^s = \\ &= \sum_{k=j+1}^n K_{\text{eff}}^{-1} \left( \frac{\dot{Q}_k}{2} \right) - \sum_{k=-n}^{j-1} K_{\text{eff}}^{-1} \left( \frac{\dot{Q}_k}{2} \right) = - \left( j - \frac{1}{2} \right) K_{\text{eff}}^{-1} \dot{Q}' \end{aligned} \quad (18)$$

Note the horizontal and vertical symmetry  $\Delta T_{j,j+1}^i = \Delta T_{j,j+1}^{-i}$  and  $\Delta T_{i,i+1}^j = \Delta T_{i,i+1}^{-j}$ .

In order to study the temperature profile, we follow the same procedure adopted by Sciacca *et al.* (2017).



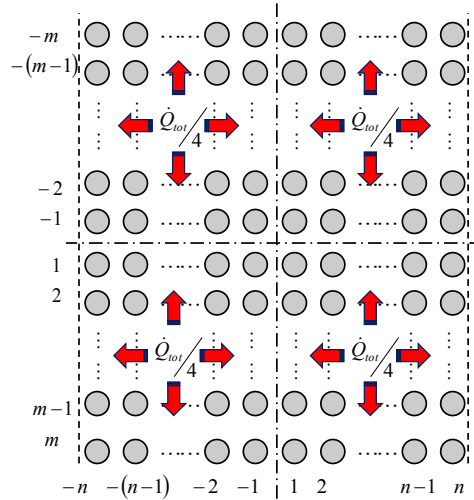


FIGURE 3. [color online] Sketch of  $2n$  columns of  $2m$  cylinders symmetrically arranged ( $n$  on the left and  $n$  on the right of the indicated vertical axis, and  $m$  on the upper and  $m$  on the lower of the indicated horizontal axis). Each cylinder radiates heat symmetrically from every side ( $\dot{Q}/4$  towards the left,  $\dot{Q}/4$  towards the right,  $\dot{Q}/4$  towards the top and  $\dot{Q}/4$  towards the bottom).

**Theorem:** According to the above assumptions, if we assume that the temperature gap  $\Delta T$  through the cylinders is  $\Delta T$  over  $\Delta x$  in the horizontal direction and  $\Delta T$  over  $\Delta y$  in the vertical direction and  $T(x, y) \in C^1(I)$  with  $I \subseteq \mathbb{R}^2$  then in the continuum they become  $dT/dx$  and  $dT/dy$ , respectively, with  $T(x, y)$  depending on both the variables, and equations (17) and (18) becomes

$$\frac{dT}{dx} = -xK_{eff}^{-1} \left( \frac{\dot{Q}'}{4} \right) \tag{19}$$

and

$$\frac{dT}{dy} = -yK_{eff}^{-1} \left( \frac{\dot{Q}'}{4} \right) \tag{20}$$

wherein the quantity  $K_{eff}^{-1} \dot{Q}'/2$  is constant.

*Proof.* The hypothesis that the temperature function  $T(x, y) \in C^1(I)$  is enough for proving the conclusion of the Theorem.  $\square$

The mathematical solution of the system (19) and (20) from  $(0, 0)$  to  $(x', y')$  is

$$T(x', y') = T(0, 0) - K_{eff}^{-1} \left( \frac{x'^2}{2} + \frac{y'^2}{2} \right) \left( \frac{\dot{Q}'}{4} \right) \tag{21}$$

where  $T(0, 0)$  is the temperature in the middle of the lattice.

If we set  $x' = n$  and  $y' = m$ , namely the cylinder at  $(n, m)$ , and we name  $T^{(\text{bath})}$  the temperature of He II just out of the lattice then we get

$$T(0,0) = T^{(\text{bath})} + (n^2 + m^2)K_{\text{eff}}^{-1} \frac{\dot{Q}}{8} \quad (22)$$

In the above discussions, it is important that the temperature  $T(0,0)$  (the maximum one in the arrays) is always smaller than the temperature  $T_\lambda$  (otherwise, helium would no longer be in the superfluid state) as well as the temperature on the walls of each cylinder.

Finally, the temperature profile, expressed in terms of  $T^{(\text{bath})}$ , is

$$T(x,y) = T^{(\text{bath})} + [(n^2 + m^2) - (x^2 + y^2)] K_{\text{eff}}^{-1} \frac{\dot{Q}}{8} \quad (23)$$

The dimensionless version of Eq. (23) is

$$\Theta(\bar{x}, \bar{y}) = 1 + \frac{C(n^2 + m^2)}{8} \left[ 1 - \left( \frac{n^2}{n^2 + m^2} \bar{x}^2 + \frac{m^2}{n^2 + m^2} \bar{y}^2 \right) \right] \quad (24)$$

where we have set  $\Theta(x,y) = \frac{T(x,y)}{T^{(\text{bath})}}$ ,  $\bar{x} = \frac{x}{n}$  and  $\bar{y} = \frac{y}{m}$ , and  $C = \frac{\dot{Q}}{K_{\text{eff}} T^{(\text{bath})}}$ . The maximum value of the temperature  $\Theta_0$  is in the middle of the system of arrays, namely at  $\bar{x} = \bar{y} = 0$ . From Eq. (22) the expression of  $\Theta_0$  is  $\Theta_0 = 1 + \frac{C(n^2 + m^2)}{8}$ , and the Eq. (24) can be written

$$\Theta(\bar{x}, \bar{y}) = 1 + (\Theta_0 - 1) \left[ 1 - \left( \frac{n^2}{n^2 + m^2} \bar{x}^2 + \frac{m^2}{n^2 + m^2} \bar{y}^2 \right) \right] \quad (25)$$

In Fig. 4 we have plotted the dimensionless temperature  $\Theta$ , (25), for  $\Theta_0 = 1.55$  (which could correspond to  $T(0,0) = 2.17$  K and  $T^{(\text{bath})} = 1.4$  K),  $n = 10$  and  $m = 20$ . Note the symmetry of the obtained paraboloid, which is due to the definition of  $\bar{x} = \frac{x}{n}$  and  $\bar{y} = \frac{y}{m}$ .

The maximum admissible value of  $\Theta$  is  $\Theta_{\text{max}} = T_\lambda / T^{(\text{bath})}$ , in order to avoid the transition to He I. This condition on  $\Theta$  sets in turn a condition on the maximum heat rate which may be extracted from the system, as expressed by a maximum of coefficient  $C_{\text{max}} = \frac{\dot{Q}_{\text{max}}}{K_{\text{eff}} T^{(\text{bath})}}$ . Since  $\Theta$  is maximum for  $\bar{x} = \bar{y} = 0$ , we thus obtain

$$\dot{Q}_{\text{max}} = \frac{8K_{\text{eff}}}{n^2 + m^2} \left[ T_\lambda - T^{(\text{bath})} \right] \quad (26)$$

This expression gives  $\dot{Q}_{\text{max}}$  as a function of  $T^{(\text{bath})}$ , of the size of the array as given by  $n$  and  $m$ , and of the geometrical features of the lattice as they appear in  $K_{\text{eff}}$ , as seen in Eqs. (7) and (9), namely, on  $c$  and  $\phi$  (the parameter  $\eta$  and  $S$  are function of  $T$ ).

## 5. Conclusions

The main results of this paper are Eqs. (7) and (9) for  $K_{\text{eff}}$  and (16) for  $\dot{Q}_{\text{max}}$  for a single cylinder and (26) for the maximum heat rate that may be extracted from the whole array as a function of its side and geometry. As it is logical to expect, and it is quantitatively confirmed by Eq. (26), the bigger the array and the lower the effective thermal conductivity  $K_{\text{eff}}$ , the lower will be the maximum bound on heat removal.

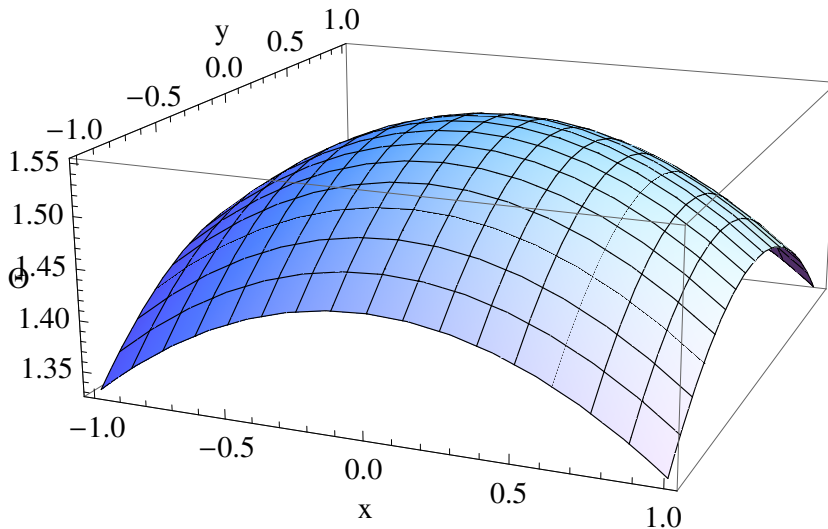


FIGURE 4. [color online] The total heat flux  $\dot{Q}$  (arrow) flowing through two consecutive cylinders in the arrays of transversal cylinders symmetrically distributed over the channel.

The current proposals for qubits are based either on neutral atoms, trapped ions, electrons spins (e.g. in quantum dots), or superconducting qubits, and one needs relatively long decoherence times, much longer than the characteristic time for the operation. To perturb the atoms as less as possible, it is convenient that the atoms are considerably heavier than helium atoms, and that helium flows spontaneously, without the external perturbations produced, for instance, by forced helium flow.

Another proposal we have made in this paper is to consider that, if some small localized turbulent region appears around the cylinders because of a local quantum thermal Reynolds number higher than the critical value, the effect of the turbulent region could be taken into account by means of an effective radius higher than the actual radius. Of course, this is an approximation, rather than a rigorous result, but since the thermal resistance of the turbulent part is much higher than the laminar one, this approximation could be acceptable. Experiments on quantum turbulence for radial heat flows around a cylinder should be done to clarify this point. Further experiments combining a longitudinal flow with the radial heat flow would also be of much interest. This illustrates how a practical problem like the one analyzed here may suggest lacking experiments of theoretical interest, still necessary for an optimization of nanorefrigeration strategies.

## Acknowledgments

D.J. acknowledges the financial support from the Dirección General de Investigación of the Spanish Ministry of Economy and Competitiveness under grant FIS2012-13370-C02-01 and TEC2015-67462-C2-2-R and of the Direcció General de Recerca of the Generalitat of Catalonia, under grant 2009 SGR-00164 and to Consolider Program Nanotherm (grant CSD-2010-00044) of the Spanish ministry of Science and Innovation. M.S. and A.S. acknowledge the hospitality of the "Group of Fisica Estadística of the Universitat Autònoma de Barcelona". M.S. and A.S. and L.G. acknowledge the financial support of the Istituto Nazionale di Alta Matematica (GNFM–Gruppo Nazionale della Fisica Matematica). LG's work is supported by Fonds National de la Recherche, Luxembourg, Grant n.7745104.

## References

- Arp, V. D. (1969). "Heat Transfer to Superfluid and Supercritical Helium". *Journal of Applied Physics* **40**, 2010. DOI: [10.1063/1.1657900](https://doi.org/10.1063/1.1657900).
- Benin, D. and Maris, H. J. (1978). "Phonon heat transport and Knudsen's minimum in liquid helium at low temperatures". *Physical Review B* **18**, 3112–3125. DOI: [10.1103/PhysRevB.18.3112](https://doi.org/10.1103/PhysRevB.18.3112).
- Bertman, B. and Kitchens, T. A. (1968). "Heat transport in superfluid filled capillaries". *Cryogenics* **8** (1), 36–41. DOI: [10.1016/S0011-2275\(68\)80051-7](https://doi.org/10.1016/S0011-2275(68)80051-7).
- Cirac, J. I. and Zoller, P. (1995). "Quantum computations with cold trapped ions". *Physical Review Letters* **74**(20), 4091. DOI: [10.1103/PhysRevLett.74.4091](https://doi.org/10.1103/PhysRevLett.74.4091).
- Di Vincenzo, D. P. (2000). "The Physical Implementation of Quantum Computation". *Fortschritte der Physik* **48** (9 -11), 771–783. DOI: [10.1002/1521-3978\(200009\)48:9/11<771::AID-PROP771>3.0.CO;2-E](https://doi.org/10.1002/1521-3978(200009)48:9/11<771::AID-PROP771>3.0.CO;2-E).
- Greywall, D. S. (1981). "Thermal-conductivity measurements in liquid  $^4\text{He}$  below 0.7K". *Physical Review B* **23**, 2152–2168. DOI: [10.1103/PhysRevB.23.2152](https://doi.org/10.1103/PhysRevB.23.2152).
- Jou, D. and Sciacca, M. (2013). "Quantum Reynolds number for superfluid counterflow turbulence". *Bollettino di Matematica Pura e Applicata* **6**, 95–103.
- Jou, D., Galantucci, L., and Sciacca, M. (2017). "Refrigeration of an Array of Cylindrical Nanosystems by Flowing Superfluid Helium". *Journal of Low Temperature Physics* **187** (5-6), 602–610. DOI: [10.1007/s10909-016-1708-4](https://doi.org/10.1007/s10909-016-1708-4).
- Jou, D., Lebon, G., and Mongiovì, M. S. (2002). "Second sound, superfluid turbulence, and intermittent effects in liquid helium II". *Physical Review B* **66** (22), 224509. DOI: [10.1103/PhysRevB.66.224509](https://doi.org/10.1103/PhysRevB.66.224509).
- Jou, D. and Mongiovì, M. S. (2006). "Description and evolution of anisotropy in superfluid vortex tangles with counterflow and rotation". *Physical Review B* **74** (5), 054509. DOI: [10.1103/PhysRevB.74.054509](https://doi.org/10.1103/PhysRevB.74.054509).
- Maris, H. J. (1973). "Dissipative coefficients of superfluid helium". *Physical Review A* **7**, 2074–2081. DOI: [10.1103/PhysRevA.7.2074](https://doi.org/10.1103/PhysRevA.7.2074).
- Mendelsohn, K. (1956). "Liquid Helium". In: *Encyclopedia of Physics*. Vol. 15. Berlin: Springer.
- Mongiovì, M. S. (1993). "Extended irreversible thermodynamics of liquid heliumII". *Physical Review B* **48**, 6276–6283. DOI: [10.1103/PhysRevB.48.6276](https://doi.org/10.1103/PhysRevB.48.6276).
- Mongiovì, M. S. and Saluto, L. (2014). "Effects of heat flux on  $\lambda$ -transition in liquid  $^4\text{He}$ ". *Meccanica* **49**, 2125–2137. DOI: [10.1007/s11012-014-9922-0](https://doi.org/10.1007/s11012-014-9922-0).
- Saluto, L. and Jou, D. (2013). "Effective thermal conductivity of superfluid helium in short channels". In: *Bollettino di Matematica Pura e Applicata*. Ed. by M. S. Mongiovì, M. Sciacca, and S. Triolo. Vol. 6. Aracne editrice, pp. 153–163.

- Saluto, L., Jou, D., and Mongiovi, M. S. (2014). “Vortex diffusion and vortex-line hysteresis in radial quantum turbulence”. *Physica B: Condensed Matter* **440**, 99–103. DOI: [10.1016/j.physb.2014.01.041](https://doi.org/10.1016/j.physb.2014.01.041).
- Saluto, L., Jou, D., and Mongiovi, M. S. (2015). “Contribution of the normal component to the thermal resistance of turbulent liquid helium”. *Zeitschrift für angewandte Mathematik und Physik* **66**(4), 1853–1870. DOI: [10.1007/s00033-015-0493-2](https://doi.org/10.1007/s00033-015-0493-2).
- Sciacca, M. and Galantucci, L. (2016). “Effective thermal conductivity of superfluid helium: laminar, turbulent and ballistic regimes”. *Communications in Applied and Industrial Mathematics* **7** (2), 111–129. DOI: [10.1515/caim-2016-0009](https://doi.org/10.1515/caim-2016-0009).
- Sciacca, M., Jou, D., and Mongiovi, M. S. (2015). “Effective thermal conductivity of helium II: from Landau to Gorter-Mellink regimes”. *Zeitschrift für angewandte Mathematik und Physik* **66**, 1835–1851. DOI: [10.1007/s00033-014-0479-5](https://doi.org/10.1007/s00033-014-0479-5).
- Sciacca, M., Sellitto, A., Galantucci, L., and Jou, D. (2017). “Refrigeration of an array of cylindrical nanosystems by superfluid helium counterflow”. *International Journal of Heat and Mass Transfer* **104**, 584–594. DOI: [10.1016/j.ijheatmasstransfer.2016.08.019](https://doi.org/10.1016/j.ijheatmasstransfer.2016.08.019).
- Sciacca, M., Sellitto, A., and Jou, D. (2014). “Transition to ballistic regime for heat transport in helium II”. *Physics Letters A* **378**, 2471–2477. DOI: [10.1016/j.physleta.2014.06.041](https://doi.org/10.1016/j.physleta.2014.06.041).
- Suominen, K.-A. (2012). “Physical Implementation of Large-Scale Quantum Computation”. In: *Handbook of Natural Computing*. Springer, pp. 1493–1520. DOI: [10.1007/978-3-540-92910-9\\_44](https://doi.org/10.1007/978-3-540-92910-9_44).
- Van Sciver, S. W. (2012). *Helium cryogenics*. Second edition. New York: Springer-Verlag. DOI: [10.1007/978-1-4419-9979-5](https://doi.org/10.1007/978-1-4419-9979-5).

---

<sup>a</sup> Universitat Autònoma de Barcelona,  
 Departament de Física,  
 08193 Bellaterra, Catalonia, Spain  
 Institut d’Estudis Catalans, Carme 47, Barcelona 08001, Catalonia, Spain

<sup>b</sup> Università di Palermo,  
 Dipartimento di Scienze Agrarie, Alimentari e Forestali,  
 Viale delle Scienze, 90128 Palermo, Italy  
 Istituto Nazionale di Alta Matematica, Roma 00185, Italy

<sup>c</sup> Università di Salerno,  
 Dipartimento di Ingegneria Industriale,  
 Campus di Fisciano, 84084, Fisciano, Italy

<sup>d</sup> Newcastle University,  
 Joint Quantum Centre (JQC) Durham–Newcastle,  
 and School of Mathematics and Statistics,  
 Newcastle upon Tyne, NE1 7RU, United Kingdom  
 Istituto Nazionale di Alta Matematica, Roma 00185, Italy

\* E-mail address: [michele.sciacca@unipa.it](mailto:michele.sciacca@unipa.it)

Paper contributed to the conference entitled “Thermal theories of continua: survey and developments (Thermocon 2016)”, which was held in Messina, Italy (19–22 April 2016) under the patronage of the *Accademia Peloritana dei Pericolanti*

Manuscript received 17 December 2017; published online 20 May 2019



© 2019 by the author(s); licensee *Accademia Peloritana dei Pericolanti* (Messina, Italy). This article is an open access article distributed under the terms and conditions of the [Creative Commons Attribution 4.0 International License](https://creativecommons.org/licenses/by/4.0/) (<https://creativecommons.org/licenses/by/4.0/>).